Effect of Milling on the Electrochemical Properties of Nanostructured Li(Fe$_{0.8}$Mn$_{0.2}$)PO$_4$ as Cathodes for Li-ion Batteries

Morteza Torabi[1,2,3,*], Alireza Tavakkoli Neyshabouri[1], Bahram SoltanMohammad[4], S.H. Razavi[2], and Mansoor Kianpour Rad[1]

[1]Materials and Energy Research Center, P.O. Box 14155-4777, Tehran, Iran
[2]Iran University of Science and Technology, P.O. Box 16846-13114, Tehran, Iran
[3]Department of Chemical Engineering and Waterloo Institute for Nanotechnology, University of Waterloo, 200 University Avenue West, Waterloo, Ontario N2L 3G1, Canada
[4]Malek-Ashtar University of Technology, P.O. Box 15875-1774, Tehran, Iran

Abstract: *Phospho-olivine Li(Fe$_{0.8}$Mn$_{0.2}$)PO$_4$ was synthesized using high-temperature solid state procedure. Ball milling was used to decrease the particle size of the active material. X-ray diffraction (XRD) confirmed formation of the phospho-olivines. The crystallite size of the ball-milled particles was calculated about 64.9 nm. Scanning electron microscopy (SEM) also showed polygonal particles of the ball-milled Li(Fe$_{0.8}$Mn$_{0.2}$)PO$_4$ and homogeneous distribution of the iron and manganese. Electrochemical evaluation of the ball-milled Li(Fe$_{0.8}$Mn$_{0.2}$)PO$_4$ demonstrated faster kinetic reaction with respect to the as-synthesized Li(Fe$_{0.8}$Mn$_{0.2}$)PO$_4$. The ball milling process led to highest capacity between the samples (150 mAh g^{-1} at 0.1 mA cm^{-2}); however, annealing the ball-milled samples showed the best cyclic performance (3% fading after 50 cycles). Ball milling process caused nanostructured Li(Fe$_{0.8}$Mn$_{0.2}$)PO$_4$ with lower diffusion length, higher electrical conductivity and higher capacity.*

Keywords: Phospho-olivines; Lithium-ion battery; Nanostructures; Ball milling

1. INTRODUCTION

Since phospho-olivines LiMPO$_4$ (M= Fe, Mn, Co, Ni) were introduced as promising cathodes for Li-ion batteries [1], a lot of research works have taken to develop and improve these materials [2-12]. Coating the particles with carbon-based materials [2], doping with multivalence cations [3] and noble metals [10] and various synthesis methods were engaged in order to increase the electrical conductivity and decrease the synthesis cost of the olivines incorporating with better performance [4-8].

The Mn and Fe based olivines are more attracted, because of their higher safety, environment friendliness, easy availability and low production costs [13, 14]. With respect to the higher capacity of the olivines when both Fe and Mn coexist at the octahedral 4c site in the olivine structure, the mixed transition metal compounds Li(Fe$_{1-y}$Mn$_y$)PO$_4$ have received more attention [2, 6-15]. Due to the larger ion radius of Mn^{2+}, substitution of Fe^{2+} by Mn^{2+} pro-

vides a wider channel for lithium diffusion into the LiFePO$_4$ structure [16]. On the other hand, reducing the particle size of the active material would be helpful to increase the electronic contact between particles without utilizing carbon and using more active material. It was shown that reducing the particle size is more important than coating particles because of low ionic conductivity of the LiMPO$_4$ conductivities respect to their electronic conductivity [17].

In this research, typical high temperature solid state reaction was utilized to obtain Li(Fe$_{0.8}$Mn$_{0.2}$)PO$_4$. Mechanical milling was applied in order to reduce the particle size and increasing the lithium ion mobility in the phosphate structure and improvement of the electrochemical properties of Li(Fe$_{0.8}$Mn$_{0.2}$)PO$_4$. Finally, the effect of annealing of the ball-milled samples was investigated.

2. EXPERIMENTAL

The Li(Fe$_{0.8}$Mn$_{0.2}$)PO$_4$ was synthesized via high-temperature method using stoichiometric ratio of NH$_4$H$_2$PO$_4$, Li$_2$CO$_3$,

*To whom correspondence should be addressed: Email: mtorabi@uwaterloo.ca
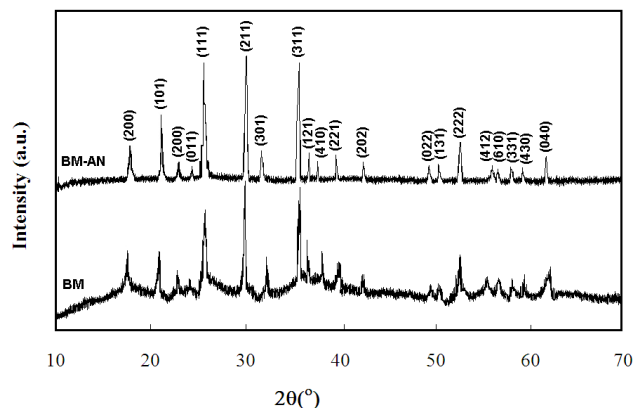Phone: +98 21 7724054, Fax: +98 21 77240480

Figure 1. XRD patterns of the ball-milled (BM) Li(Fe$_{0.8}$Mn$_{0.2}$)PO$_4$ and annealed ball-milled (BM-AN) samples.

FeC$_2$O$_4$.2H$_2$O and MnCO$_3$. The process was performed in a high purity (5N) nitrogen flow at 750 °C for 24 h. Milling (SPEX3000) was done for 30min. The samples obtained in this process are hereafter named AS (as-synthesized) and BM (ball milled). Annealing of the ball milled sample also was done in a tube furnace under argon for 24 h at 600°C (named as BM-AN).

The morphology of the olivine nanostructures was studied using scanning electron microscopy (SEM, VEGA, TESCAN). The structural characterization of powders was carried out by analyzing the X-ray diffraction patterns obtained using a Unisuntis (XMD 300) diffractometer (λ=1.5405 Å for CuKα radiation). Electrical conductivity measurements were done using four-probe method at room temperature (Keithley 2420).

The cathodes were prepared by mixing active material (85 wt%) with polyvinylidene fluoride (PVDF) (5 wt%), and carbon black (10 wt%) in N-methyl-2-pyrrolidione (NMP) solvent. The working electrolyte was 1M LiBF$_4$ in a 50:50 (v/v) mixture of ethylene carbonate (EC) and dimethyl carbonate (DMC). The 2032 coin cells were assembled in glove box under Ar atmosphere with a Li-metal disk as the negative electrode. The cells were galvanostatically charged and discharged in the range of 2-4.5 V at a constant current density of 0.1 mA cm^{-2}. Cyclic voltammetry measurements were performed at a scanning rate of 0.1 mV s^{-1}. All electrochemical measurements were carried out using an Autolab PGSTAT30.

3. RESULTS AND DISCUSSION

Fig. 1 illustrates XRD patterns of the samples prepared via solid state reaction method. The crystal structure of AS, BM and BM-AN samples demonstrate a single-phase olivine-type orthorhombic *Pnma* structure. Ball milling and annealing did not affect the crystal structure of the AS sample. Only a broadening and decreasing of intensity were detected in all diffraction peaks for BM sample. The peaks are sharpen and clear with lower base for the BM-AN which shows highly crystalized Li(Fe$_{0.8}$Mn$_{0.2}$)PO$_4$. The average crystallite sizes of the samples AS, BM and BM-AN were calculated about 750.6, 64.9 and 163.7 nm, respectively, according to XRD-Scherrer formula (Eq. (1)):
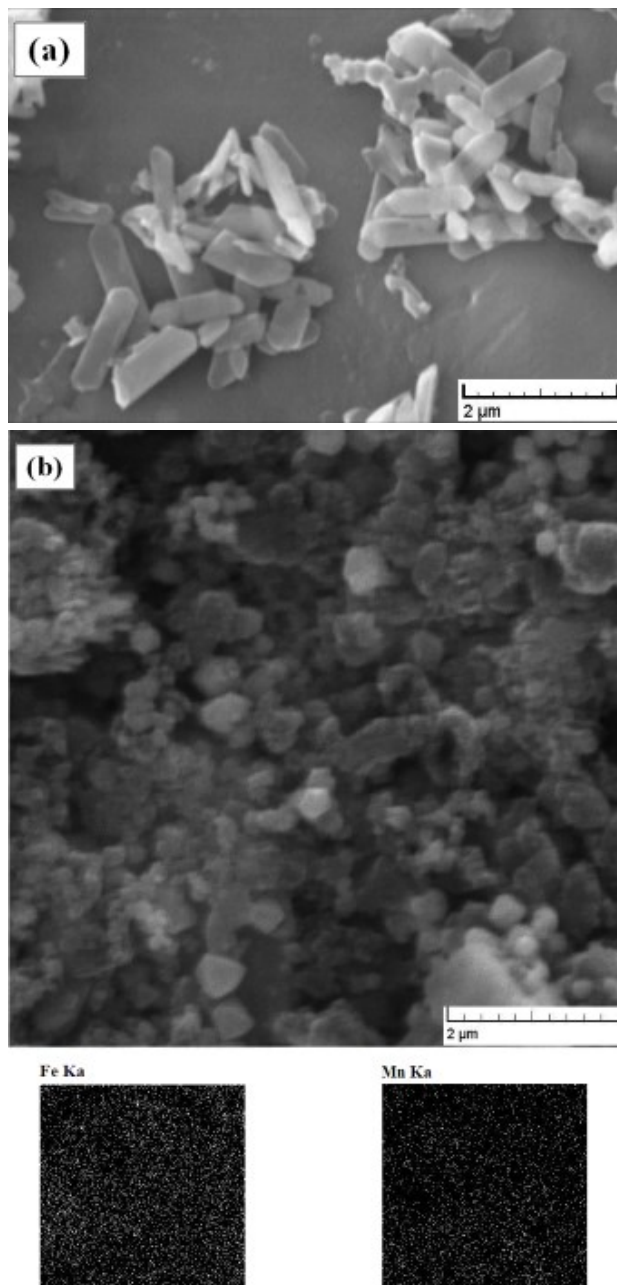
$$d = \frac{k\lambda}{B\cos\theta} \qquad (1)$$

Figure 2. SEM images of the (a) as synthesized (AS) and (b) ball-milled (BM) samples with elemental mapping.

where d is the mean crystallite size, k a constant usually equals to ~0.9, λ the wavelength of Cu Kα (λ = 1.5405 Å), B the full width at half maximum intensity of the peak (FWHM) in radian and θ is Bragg's diffraction angle [18]. Such fine crystallite size leads to broads and weak peaks in the XRD pattern for the BM.

Fig. 2 shows SEM images of the AS and BM samples. AS powders consist of hexagon particles with a particle sizes of about 1-2 µm. The morphology of the BM particles is polygonal that are formed during milling process. Elemental mapping of the samples also represent homogeneous distribution of the iron and manganese.
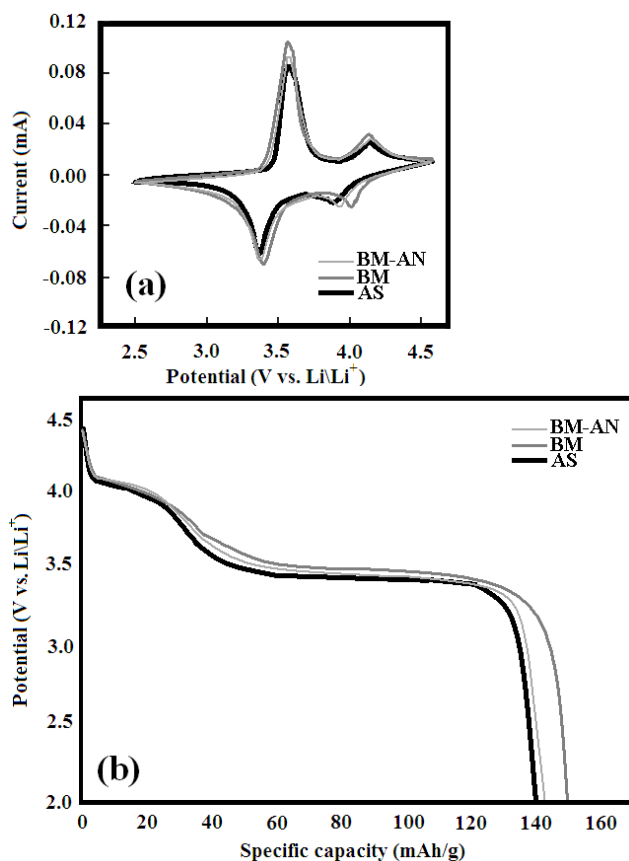
Figure 3. (a) First cyclic voltammogram and (b) First discharge curve of the AS, BM and BM-AN samples.

Figure 4. Cyclic performance of the AS, BM and BM-AN samples.

First charge/discharge voltammogram curves are presented in Fig. 3(a) for three samples. Two couples of oxidation/reduction peaks could be detected during each voltammogram. The iron oxidation and reduction peaks were emerged at 3.53 and 3.37 V for AS sample, respectively. Also, the oxidation and reduction peaks of the manganese were arisen at 4.12 and 3.87 V. The oxidation and reduction of the iron were occurred at 3.52 and 3.41 for BM sample. Manganese oxidation and reduction peaks were observed at 4.11 and 4.02, as well. Sharper peaks for BM sample indicate higher diffusion rate of the Li ion in respect of the AS because of the smaller particles of the sample BM. With integration of the voltammogram specific capacity of the samples could be obtained which is 151, 139 and a143 for BM, AS and BM-AN samples, respectively. The larger difference between the anodic and cathodic potential of the peaks (ΔEp) for AS sample in respect of BM sample mentioned a kinetic limitation in the electrochemical process. On the other hand, the significant difference is due to the nanostructure of the BM particles that provides more active surface during electrochemical reaction and increases the efficiency of the active material. Cyclic voltammogram of BM-AN sample showed improved kinetic performance respect to AS sample. It had lower capacity than BM but higher than AS.

The discharge curves of samples AS, BM and BM-AN at 0.1 mA cm^{-2} are presented in Fig. 3(b). Two distinct plateaus can be ob-
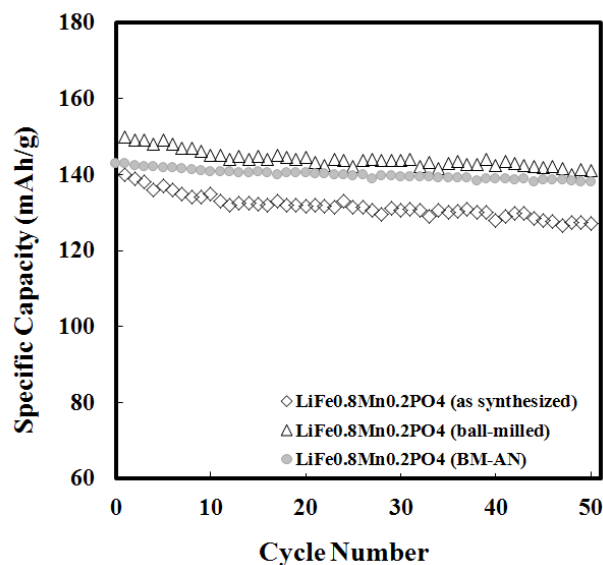
served at about 3.4 and 4.0 V for AS, BM and BM-AN, which correspond to the intercalation of lithium ions to (Fe$_{0.8}$Mn$_{0.2}$)PO$_4$ at these voltage regions for Fe^{3+}/Fe^{2+} and Mn^{3+}/Mn^{2+} couples. Such discharging behavior corresponds well with the results of the CV analysis. The discharge capacity of AS was obtained 140 mAh g^{-1} which corresponds to about 82% utilization of the active material. The discharge capacity is 150 and 143 mAh g^{-1} for BM and BM-AN samples, respectively.

Fig. 4 demonstrates the cycling performance of the samples at 0.1 mA cm^{-2}, studied over 50 charge/discharge cycles. The capacity is lowest for AS; however, it shows almost stable cycling property. The capacity fading of the AS and BM were 5% and 3% over 10 cycles. The capacity of the AS and BM after 50 cycles reached to 127 and 141 mAh g^{-1}, respectively with 9% and 6% capacity fading. The BM-AN sample shows the best cyclic performance. It has lower capacity respect to the BM, but has more stability over cycling. For this sample, the fading is less than 3% after 50 cycles and reached to 138 mAh g^{-1} after 50 cycles. The first cycle capacity of the BM is highest, but microscopic disorders and dislocations associated with the sample limited the cyclability of the ball-milled Li(Fe$_{0.8}$Mn$_{0.2}$)PO$_4$ respect to the ball-milled sample after a soft annealing.

Table 1 compares the electrical conductivity of the samples with selected data from literatures [3, 19-23]. The electrical conductivity at room temperature is in the range of 10^{-9} S cm^{-1} for LiFePO$_4$ [3] while for LiMnPO$_4$ is less than 10^{-10} S cm^{-1} [19]. The electrical conductivity of LiFe$_{0.45}$Mn$_{0.55}$PO$_4$ is higher than 10^{-9} and for Li-Fe$_{0.25}$Mn$_{0.75}$PO$_4$ is higher than 10^{-10} S cm^{-1} [21]. It is represented that LiFe$_{0.8}$Mn$_{0.2}$PO$_4$ has the highest conductivity about 3.46×10^{-5} S cm^{-1} between all LiFe$_{1-x}$Mn$_x$PO$_4$ (x≤0.3) [22]. With use of Fe$_2$P, the conductivity of the LiFe$_{0.9}$Mn$_{0.1}$PO$_4$ increased to higher than 10^{-4} S cm^{-1} [23].

The electrical conductivity of the AS-LiFe$_{0.8}$Mn$_{0.2}$PO$_4$ is 1.88×10^{-9} (S cm^{-1}) which caused slow kinetic performance and low

capacity. Decreasing the particle size by ball-milling led to higher electrical conductivity about two orders for BM (2.44×10^{-7} S cm^{-1}). Annealing the samples again decreased the conductivity about one order (1.93×10^{-8} S cm^{-1} for BM-AN). It had shown already that ionic conductivity dominates the overall conductivity of the olivine LiFePO$_4$ and lowering the particle size associates with higher ionic conductivity and hence, better electrochemical performance [17]. It was shown that the ionic conductivity of the LiFePO$_4$ and Mn-substituted LiFePO$_4$ are the same due to their same activation energy [21]. Ball milling solely increased the electrochemical performance of the LiFe$_{0.8}$Mn$_{0.2}$PO$_4$ by improving the ionic and eventually electrical conductivity of the phosphate; however, cyclability was scarified. Annealing improved the cyclic work performance and has higher capacity than AS sample.

4. CONCLUSION

Ball milling led to breaking the hexagonal Li(Fe$_{0.8}$Mn$_{0.2}$)PO$_4$ microparticles to nanoparticles, increment of the active surface and lowering the diffusion length. SEM images showed that the nanocrystalline Li(Fe$_{0.8}$Mn$_{0.2}$)PO$_4$ has polygonal morphology with crystallite size of about 64.9 nm. Elemental mapping of the samples also represented homogeneous composition of the olivine. Cyclic voltammograms showed better performance of the ball-milled sample with respect to the as-synthesized sample. Specific capacities of the ball-milled and as-synthesized samples were about 150 and 140 mAh g^{-1}, respectively. Annealing of Li(Fe$_{0.8}$Mn$_{0.2}$)PO$_4$ after ball milling resulted in reduction of capacity while the capacity retention improved. Increasing the conductivity of the ball-milled sample caused by decreasing the particle size led to faster kinetic processes and higher capacity. Therefore, it can be concluded that with decreasing the particle size, the electrical conductivity increases due to faster ionic transportation via particles and faster electrochemical kinetic process and higher capacity. However, the dislocations and microscopic defects of the broken particles accelerate capacity fading. Hence, annealing the ball-milled particles decreases the fading of the reversible capacity significantly.

REFERENCES

[1] A.K. Padhi, K.S. Nanjundaswamy, J.B. Goodenough, J. Electrochem. Soc., 144, 1188 (1997).

[2] C.H. Mi, X.G. Zhang, X.B. Zhao, H.L. Li, Mater. Sci. Eng. B, 129, 8 (2006).

[3] S. Chung, J. Bloking, Y. Chiang, Nat. Mater., 2, 123 , (2002).

[4] R. Dominko, M. Bele, M. Gaberscek, M. Remskar, D. Hanzel, J.M. Goupil, S. Pejovnik, J. Jamnik, J. Power Sources, 153, 274 (2006).

[5] S. Yang, P.Y. Zavalij, M.S. Whittingham, Electrochem. Commun., 3, 505 (2001).

[6] L. Wang, Y. Huang, R. Jiang, D. Jia, Electrochim. Acta, 52, 6778 (2007).

[7] B. Wang, Y. Qiu, S. Ni, Solid State Ionics, 178, 843 (2007).

[8] M. Zhang, L.F. Jiao, H.T. Yuan, Y.M. Wang, J. Guo, M. Zhao, W. Wang, X.D. Zhou, Solid State Ionics, 177, 3309 (2006).

[9] D. Jugović, D. Uskoković, J. Power Sources, 190, 568 (2009)

[10] M. Talebi-Esfandarani, O. Savadogo, J. Appl. Electrochem., 44, 555 (2014).

[11] J. Triwibowo, E. Yuniarti, E. Suharyadi, AIP Conference Proceedings, 1617, 52 (2014).

[12] Y. Wang, G. Cao, Adv. Mater., 20, 2251, (2008).

[13] A. Yamada, S.C. Chung, J. Electrochem. Soc., 148, A960 (2001).

[14] A. Yamada, Y. Kudo, K.Y. Liu, J. Electrochem. Soc., 148, A1153 (2001).

[15] G. Li, H. Azuma, M. Tohda, J. Electrochem. Soc., 149, A743 (2002).

[16] K. T. Lee, K. S. Lee, J. Power Sources, 189, 435 (2009).

[17] M. Gaberscek, R. Dominko, J. Jamnik, Electrochem. Commun., 9, 2778 (2207).

[18] B.D. Cullity, Elements of X-ray Diffraction, 2nd ed., Addison-Wesley, London, 1978.

[19] C. Delacourt, L. Laffont, R. Bouchet, C. Wurm, J.-B. Leriche, M. Morcrette, J.-M. Tarascon, C. Masquelier, J Electrochem. Soc., 152, A913 (2005).

[20] M. R. Roberts, G. Vitins, G. Denuault, J. R. Owena, J. Electrochem. Soc., 157, A381 (2010).

[21] J. Molenda, W. Ojczyk, J. Marzec, J. Power Sources, 174, 689 (2007).

[22] Y. Wang, D. Zhang, X. Yu, R. Cai, Z. Shao, X. Liao, Z. Ma, J Alloys Comp., 492, 675 (2010).

[23] K. T. Lee, K. S. Lee, J. Power Sources, 189, 435 (2009).

Table 1. Comparison of electrical conductivity for this work with the previous reports for the phosphate cathodes.

	Electrical Conductivity (S cm^{-1} at 298 K)	Reference
LiFePO$_4$	10^{-9}-10^{-10}	[3]
LiMnPO$_4$	3×10^{-9} (at 573 K) est. 1.2×10^{-20}	[19, 20]
Li-Fe$_{0.25}$Mn$_{0.75}$PO$_4$	$>10^{-10}$	[21]
LiFe$_{0.45}$Mn$_{0.55}$PO$_4$	$>10^{-9}$	[21]
Li-Fe$_{0.9}$Mn$_{0.1}$PO$_4$	2.63×10^{-7}	[22]
Li-Fe$_{0.8}$Mn$_{0.2}$PO$_4$	3.46×10^{-5}	[22]
Li-Fe$_{0.7}$Mn$_{0.3}$PO$_4$	3.96×10^{-6}	[22]
LiFe$_{0.9}$Mn$_{0.1}$PO$_4$/Fe$_2$P	2.72×10^{-4}	[23]
AS (as-synthesized Li-Fe$_{0.8}$Mn$_{0.2}$PO$_4$)	1.88×10^{-9}	This work
BM (ball-milled Li-Fe$_{0.8}$Mn$_{0.2}$PO$_4$)	2.44×10^{-7}	This work
BM-AN (annealed ball-milled Li-Fe$_{0.8}$Mn$_{0.2}$PO$_4$)	1.93×10^{-8}	This work